Molecular Therapy
Methods & Clinical Development
Original Article

Pooled Screens Identify *GPR108* and *TM9SF2* as Host Cell Factors Critical for AAV Transduction

W. Hans Meisen,[1] Zahra Bahrami Nejad,[1] Miki Hardy,[1] Huiren Zhao,[1] Oliver Oliverio,[1] Songli Wang,[1] Christopher Hale,[1] Michael M. Ollmann,[1] and Patrick J. Collins[1]

[1]Genome Analysis Unit, Amgen Research, South San Francisco, CA, USA

Adeno-associated virus (AAV) has been used extensively as a vector for gene therapy. Despite its widespread use, the mechanisms by which AAV enters the cell and is trafficked to the nucleus are poorly understood. In this study, we performed two pooled, genome-wide screens to identify positive and negative factors modulating AAV2 transduction. Genome-wide libraries directed against all human genes with four designs per gene or eight designs per gene were transduced into U-2 OS cells. These pools were transduced with AAV2 encoding EGFP and sorted based on the intensity of EGFP expression. Analysis of enriched and depleted barcodes in the sorted samples identified several genes that putatively decreased AAV2 transduction. A subset of screen hits was validated in flow cytometry and imaging studies. In addition to *KIAA0319L* (*AAVR*), we confirmed the role of two genes, *GPR108* and *TM9SF2*, in mediating viral transduction in eight different AAV serotypes. Interestingly, *GPR108* displayed serotype selectivity and was not required for AAV5 transduction. Follow-up studies suggested that GPR108 localized primarily to the Golgi, where it may interact with AAV and play a critical role in mediating virus escape or trafficking. Cumulatively, these results expand our understanding of the process of AAV transduction in different cell types and serotypes.

INTRODUCTION

Adeno-associated viral (AAV) vectors are one of the most actively investigated gene therapies. Recently, the AAV vectors voretigene neparvovec and onasemnogene abeparvovec were approved by the US Food and Drug Administration (FDA), and there are more than 20 ongoing phase 3 clinical trials utilizing AAV vectors for gene therapy (https://clinicaltrials.gov/). Despite these advances in the clinic and promising research in vector engineering, many aspects of AAV biology remain unknown. For example, although several naturally existing serotypes have been identified and characterized for their ability to differentially infect various tissues, there has been considerable debate as to the entry receptors for these serotypes as well as the role that those factors might play in conferring tissue specificity. Recently, *KIAA0319L* (*AAVR*) was identified in a 2016 study by Pillay et al.[1] as a factor required for transduction in many AAV serotypes. Follow-up studies detailing *KIAA0319L*'s interactions with AAV2 and other serotypes have been published, but other host cell factors essential for AAV transduction remain elusive.[2]

KIAA0319L was identified in a genome-wide, insertional mutagenesis screen using the haploid HAP1 cell line.[1] Similar haploid genetic screens with modified selection strategies have been utilized to identify host cell factors important for vaccinia virus, Chikungunya virus, influenza virus, and other viral infections.[3–5] While representing an effective research tool, these screens have several limitations, including an inability to assess the perturbation of genes in diploid regions of the genome, an integration bias of transposons or viruses, and challenges in maintaining haploidy in cell cultures over time.[6,7]

CRISPR screens have emerged as an important research tool that can overcome some of the limitations of haploid insertional mutagenesis screens. CRISPR technology enables screening in a variety of cell lines/types utilizing targeted libraries to perturb virtually any locus in the genome. To identify host cell factors essential for AAV transduction, we conducted two independent, genome-wide CRISPR screens in the non-haploid U-2 OS cell line and compared the overlap between these two pooled screens with published data from the Pillay et al.[1] haploid mutagenesis screen. We validated a selection of the overlapping genes from the CRISPR screens and identified at least one gene, *GPR108*, that, when perturbed, displays serotype specificity. We explored the subcellular localization of GPR108 and its potential interactions with AAV and discussed the possible mechanisms by which *GPR108* may influence AAV transduction. Taken together, these results expand our understanding of the process of AAV transduction for a variety of cell types and serotypes.

RESULTS

CRISPR-Cas9 Screens Identify Genes that Modulate AAV2 Transduction in U-2 OS Cells Independent from Fitness

To identify host cell factors modulating AAV2 transduction, we performed a set of pooled CRISPR-Cas9 screens in U-2 OS cells, a permissive cell type for viral transduction. Similar to the Pillay et al.[1] strategy, we chose to use an AAV2 vector encoding EGFP to enable fluorescence-based cell sorting and to function as a surrogate marker for successful virus transduction. Using this approach, the

Received 20 February 2020; accepted 12 March 2020;
https://doi.org/10.1016/j.omtm.2020.03.012.

Correspondence: Patrick Collins, Genome Analysis Unit, Amgen Research, 1120 Veterans Boulevard, South San Francisco, CA 94080, USA.
E-mail: pcolli01@amgen.com

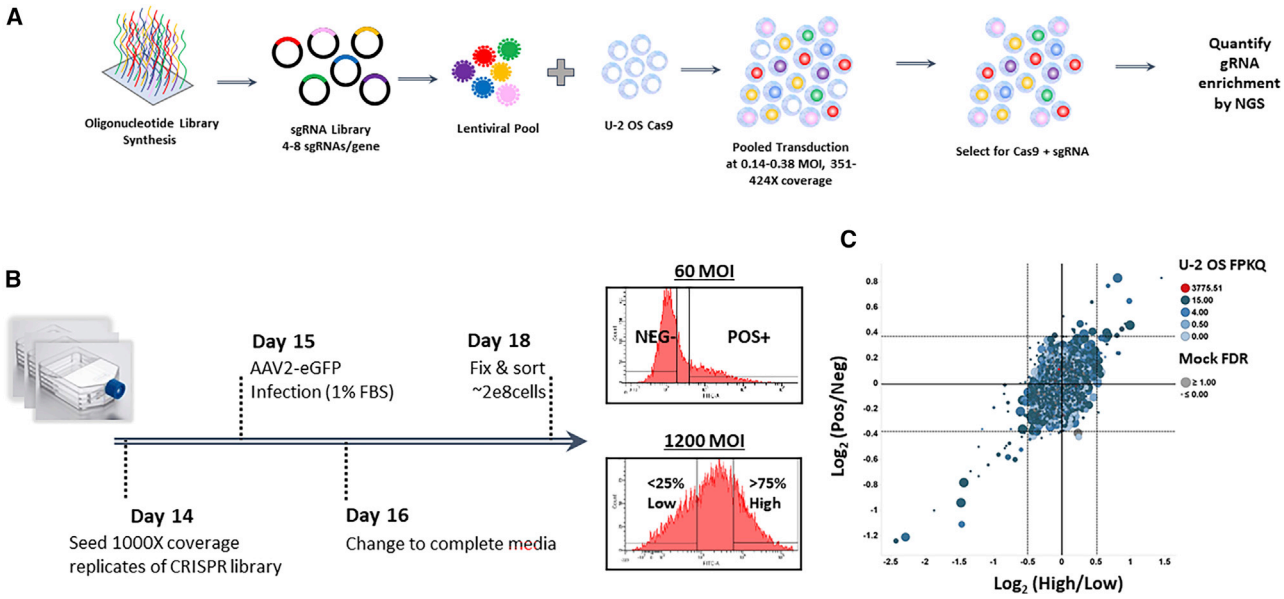

Figure 1. Summary of AAV CRISPR Screen Design and Optimization

(A) Overview of CRISPR library generation, target cell transduction, and sgRNA enrichment. (B) Experimental design and sorting schemes for AAV2-EGFP transduction of CRISPR libraries in U-2 OS Cas9 cells. (C) Comparison of the gene-aggregated $\log_2$ ratios of sgRNA abundance in the high and low EGFP populations from the 1,200 MOI transduction (x axis) and the positive and negative populations from the 60 MOI transduction (y axis). The color of each dot is related to its expression in U-2 OS cells and the size proportional to the FDR in the comparison of the mock transduction to the plasmid library. The lines indicate the mean (solid) and three standard deviations (dotted) of all genes in each screen.

knockout (KO) of genes required for AAV transduction would theoretically result in no or low EGFP expression when treated with AAV2-EGFP, while genes that limit AAV transduction would potentially result in increased EGFP expression when knocked out. Prior to expanding our screen to the entire genome, we conducted a pair of pooled screens targeting roughly 6,000 genes (using eight single guide RNAs [sgRNAs] per gene) to optimize the multiplicity of infection (MOI) for AAV2 and the cell sorting strategy. We evaluated two different MOIs and sorting approaches to identify cells with perturbations conferring the most and least permissive states for AAV transduction (Figure 1). A low 60 MOI condition resulted in approximately 25% of cells becoming EGFP positive, and these cells were sorted to capture both EGFP-positive and EGFP-negative populations. A higher, 1,200 MOI condition resulted in nearly the entire population becoming EGFP positive, and we subsequently isolated the top and bottom quartile of EGFP-expressing cells (high/low). Individual sgRNA abundance in each sorted sample was determined by next-generation sequencing (NGS) and expressed as the $\log_2$ ratio of normalized counts for the positive EGFP population over the negative population (pos/neg) or the high EGFP population over the low EGFP population (high/low). A comparison of aggregated gene-level results from the two conditions revealed a reasonable correlation (Pearson's r = 0.4) in the $\log_2$ ratios of individual genes, although this trend was more pronounced for clear outliers. Analysis of each condition identified 36 genes with significantly altered ratios in the pos/neg condition compared to 99 genes in the high/low condition using the same false discovery rate (FDR) cutoff of 0.05 (Table S1). Based on the results of this pilot screen, we proceeded to interrogate the remainder of the genome using the higher MOI and high/low sorting strategy.

Ultimately, we performed genome-wide screens with two different CRISPR libraries: the first with ~155,000 (155K) elements averaging eight sgRNAs per gene spread across three separate modules, and the second with a single 80,000 (80K) element library averaging four sgRNAs per gene. As most genes would not be expected to have a role in AAV2 transduction, we found that the gene-aggregated $\log_2$ ratios from the two screens were poorly correlated (Pearson's r = 0.11) (Figure 2A). However, direct comparison of sgRNA abundance in the high sort to the low sort revealed a number of genes in both screens that were significantly altered in the high EGFP population relative to the low population. As others have found, the FDRs for the 80K library, with fewer sgRNAs per gene, needed to be relaxed compared to the 155K library to detect a similar number of genes with significantly altered abundance despite the fold change of individual sgRNAs and gene-level aggregates being similar between the two libraries (Figure 2B).[8] Applying a FDR cutoff of 0.05 to the 155K screen and 0.2 to the 80K screen resulted in the detection of 61 and 7 genes that were enriched in the high sort and/or depleted in the low sort, respectively. Between the two screens, there was no overlap in genes that, when knocked out, increase AAV transduction (Table S2). Using the same cutoffs, we identified 73 and 36 genes that were either enriched in the low sort and/or depleted in the high sort (Table S2), including eight genes that were found in both screens. Ordered from the greatest to

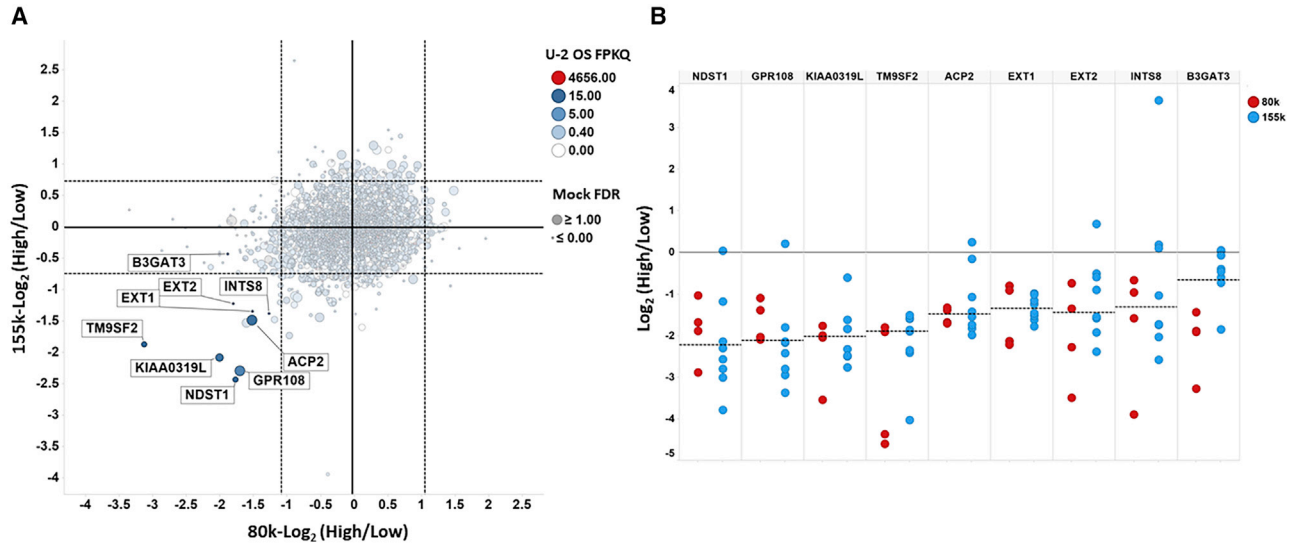

Figure 2. Two Genome-wide CRISPR Screens Identify Genes Important for AAV Transduction

(A) Comparison of the gene-aggregated $\log_2$ ratios of sgRNA abundance for the high and low EGFP populations from a 1,200 MOI transduction of U-2 OS Cas9 cells harboring an 80K CRISPR library (x axis) or a 155K CRISPR library (y axis). The color of each dot is related to its expression in U-2 OS cells and the size proportional to the FDR in the comparison of the mock transduction to the plasmid library. The lines indicate the mean (solid) and three standard deviations (dotted) of all genes in each screen. (B) Individual $\log_2$ ratios of sgRNA abundance in the high and low EGFP populations for significant, overlapping genes in the 80K library (red) or 155K library (blue).

weakest effect size in the 155K screen, these genes were *NDST1*, *GPR108*, *KIAA0319L*, *TM9SF2*, *ACP2*, *INTS8*, *EXT1*, *EXT2*, and *B3GAT3* (Table 1). While these genes are likely to be required for AAV transduction, to rule out the decrease in abundance of sgRNAs against these genes being attributable to diminished viability, we assessed the fitness impact by comparing sgRNA abundance in a mock transduction to the initial value in the libraries. We found that sgRNAs for *INTS8*, *EXT1*, *EXT2*, and *B3GAT3* were significantly depleted relative to the initial library in both screens, suggesting that deletion of these genes may impact cell fitness.

GPR108 and *TM9SF2* Are Factors Critical for AAV2 Transduction

Based on overlap between the Pillay et al.[1] screen and the two CRISPR screens, *GPR108*, *TM9SF2*, *NDST1*, *HS6ST1*, *SLC45A3*, and *SLC35B2* were selected for further validation. While the latter three genes were not significant in both of the CRISPR screens, they were selected for follow-up because they were significant in at least one screen and generally appeared to negatively impact AAV transduction when perturbed in both screens. Stable KO cell lines were generated in U-2 OS cells transduced with an all-in-one lentiviral vector expressing both a sgRNA and Cas9. Two cell lines with different sgRNAs were generated for each gene, and gene editing rates were determined by Inference for CRISPR edits (ICE) analysis (Tables S3 and S4).[9] Gene KO in these cells did not appear to negatively impact cell growth (Figure S1). For the initial validation assays, cell lines were transduced with AAV2 encoding EGFP for 3 days, fixed, and imaged. In these experiments parental cells were used as a positive control for AAV transduction, and *KIAA0319L* (*AAVR*) KO cells were used as a negative control for transduction.[1] Compared to parental cells, the KO of *GPR108* significantly reduced the EGFP intensity by 8.1- and 7.3-fold in each KO cell line (Figure 3A). This reduction in EGFP intensity was similar to *KIAA0319L* KO cells (6.2-fold). KO of *TM9SF2* and *NDST1* reduced EGFP intensity an average of 4.6- and 3.4- fold, respectively. Additional genes evaluated showed moderate or no reductions in EGFP intensity (Figure 3A). In agreement with the EGFP intensity data, the percentage of EGFP-positive cells in these KO cells was also significantly reduced compared to the parental cells ($p < 0.0001$ by ANOVA with Dunnett's multiple comparisons tests). An average of 29.5%, 30.4%, 49.2%, and 41.7% of *GPR108*, *TM9SF2*, *NDST1*, and *KIAA0319L* KO cells, respectively, were EGFP positive compared to 99.5% of the parental cells (Figures 3B and 3C).

GPR108 and *TM9SF2* Modulate AAV Transduction in Multiple Serotypes

The pooled screen and initial validation assays were performed with AAV2-EGFP. We next evaluated the role of *GPR108*, *TM9SF2*, and *NDST1* in modulating transduction of multiple AAV serotypes. Parental and KO cell lines were transduced with eight different serotypes of AAV encoding EGFP. A higher MOI was used for these studies to account for differences in the *in vitro* transduction of these serotypes. As in the previous experiments, parental U-2 OS cells were used as a positive control and *KIAA0319L* (*AAVR*) KO cells were used as a negative control. The transduction efficiency varied between 4.7% and 100% across the different serotypes (Figure S2). Despite these differences, KO of *KIAA0319L*, *TM9SF2*, and *GPR108* significantly reduced the number of EGFP-positive cells compared to parental U-2 OS controls in AAV1, AAV2, AAV5 (*TM9SF2* and *KIAA0319L* only), AAV6, AAV7, AAV8, AAV9, and AAVDJ. Compared to parental cells, *KIAA0319L*, *GPR108*, and *TM9SF2* KO cells reduced AAV transduction an average of 3.7-, 3.1-, and 2.5-fold across all

Table 1. Overlapping Genes with Significantly Altered sgRNA Abundance in Both CRISPR Genome-wide Screens

Gene	Module	155K Log_2 (High/Low)	155K High/Low FDR	155K (Mock/Plasmid)	155K Mock FDR	80K Log_2 (High/Low)	80K High/Low FDR	80K (Mock/Plasmid)	80K Mock FDR	U-2 OS FPKQ
NDST1	1	−2.4	1.0E−14	−0.3	4.2E−01	−1.8	3.2E−02	−0.5	4.4E−01	43.5
GPR108	1	−2.3	1.9E−14	−0.1	8.5E−01	−1.7	3.8E−02	−0.1	1.0E+00	9.3
KIAA0319L	3	−2.1	1.3E−08	0.2	1.0E+00	−2.0	4.8E−03	−0.3	7.4E−01	12.8
TM9SF2	1	−1.9	1.4E−17	−0.4	5.6E−02	−3.1	1.9E−03	−0.2	4.8E−01	29.7
ACP2	1	−1.5	9.9E−08	−0.1	1.0E+00	−1.5	5.6E−02	0.2	1.0E+00	13.6
INTS8	3	−1.4	5.8E−03	−2.1	3.4E−06	−1.3	1.1E−01	−1.0	2.8E−02	8.1
EXT1	1	−1.3	1.2E−12	−1.0	5.4E−04	−1.5	1.0E−01	−1.0	9.8E−03	41.2
EXT2	1	−1.2	1.2E−06	−0.7	9.7E−03	−1.8	3.6E−02	−0.9	3.6E−02	45.8
B3GAT3	1	−0.4	3.6E−02	−1.0	4.4E−05	−1.9	1.1E−02	−0.6	3.4E−02	12.9

FDR, false discovery rate; FPKQ, fragments per kilobase per million sequenced × quantile multiplier.

serotypes, respectively (*GPR108* excludes AAV5) (Figure S2). An analysis of the EGFP intensity from these studies showed similar results. Compared to parental cells, *KIAA0319L*, *GPR108*, and *TM9SF2* KO cells reduced EGFP intensity an average of 6.9-, 5.3-, and 3.6-fold, respectively (*GPR108* excludes AAV5) (Figure 4). While the percentage of EGFP-positive cells in *NDST1* KO cells was not reduced across the serotypes tested, the EGFP intensity was significantly decreased by an average of 55.6% and 47.3% in *NDST1* KO cells treated with AAV2 ($p < 0.0001$) or AAVDJ ($p < 0.0001$), respectively (Figure 4). These results suggested at high MOIs *NDST1* may potentiate AAV transduction of certain serotypes, but it may not be required for successful AAV transduction. To further explore the relationship between MOI and *NDST1* in virus transduction, we treated KO cells with AAV2-EGFP at a range of MOIs and evaluated changes in EGFP intensity and the percentage of EGFP-positive cells compared to parental cells. At low MOIs, we observed that *NDST1* KO reduced the percentage of EGFP-positive cells, while at high MOIs, all of the KO cells were EGFP positive but the EGFP intensity was decreased (Figure S3). These results indicate that *NDST1* is important for AAV transduction, but its role may be MOI-dependent and it is not required at high MOIs for successful transduction of certain AAV serotypes.

AAV5 Does Not Require *GPR108* for Viral Transduction

The KO of *GPR108* significantly inhibited virus-mediated EGFP transduction across seven different AAV serotypes. Interestingly, transduction of *GPR108* KO cells with AAV5-EGFP achieved similar levels of EGFP expression as parental cells (average of *GPR108* KO cell lines 33.8% EGFP positive versus parental cells 35.6% EGFP positive). This observation was unique to *GPR108*, as AAV5 transduction was reduced an average of 3.2- and 3.3-fold in *TM9SF2* and *KIAA0319L* KO cells, respectively (Figures 4 and 5A). These results were also confirmed in flow cytometry experiments. In these assays, AAV5-EGFP transduction of *GPR108* KO cells resulted in EGFP expression levels similar to parental cells (average of *GPR108* KO cell lines 44.9% EGFP positive versus parental cells 36.1% EGFP positive) (Figure S4). To determine whether this observation would translate to another cell line, the study was repeated with the human hepatocellular carcinoma cell line HEP3B. *GPR108*, *TM9SF2*, and *KIAA0319L* KO cells were generated via co-transfection with Cas9 and a pool of three sgRNAs and the KO efficiency of these cells was confirmed via ICE analysis (Table S5). Following successful gene KO, cells were transduced with AAV2-EGFP or AAV5-EGFP for 48 h. Similar to findings in U-2 OS cells, AAV2 transduction was significantly reduced upon *KIAA0319L*, *TM9SF2*, and *GPR108* gene KO. The percentage of EGFP-positive cells decreased from 36.7% in the parental cells to 3.9%, 4.3%, and 15.0% in the *KIAA0319L*, *GPR108*, and *TM9SF2* KO cells, respectively (Figure 5B). Transduction of HEP3B cells with AAV5-EGFP reduced transduction percentages in *KIAA0319L* (1.3% EGFP positive) and *TM9SF2* (1.1% EGFP positive) compared to the parental cells (4.8% EGFP positive). However, we observed no decrease in the percentage of EGFP-positive cells in *GPR108* KO cells (6.3%) (Figure 5B).

GPR108 Overexpression Does Not Enhance AAV Transduction and Cannot Compensate for Loss of *KIAA0319L* (*AAVR*) in U-2 OS Cells

Given the unique observations with *GPR108*, we further explored its role in AAV transduction and its potential relationship with *KIAA0319L* (*AAVR*). We generated a construct encoding wild-type (WT) *GPR108* with a C-terminal FLAG-tag (Figure 6C). The construct was packaged into a lentiviral vector and used to generate stable cell lines. We first evaluated whether the FLAG-tagged version of *GPR108* was capable of rescuing AAV2 transduction in a *GPR108* KO pool. In these assays, KO of *GPR108* in U-2 OS cells reduced AAV2-delivered EGFP intensity by 6.5-fold ($p < 0.0001$), but this decrease could be rescued in *GPR108* KO cells stably expressing the WT *GPR108*-FLAG construct (Figures 6A and 6B). We next evaluated the ability of *GPR108* overexpression to enhance AAV transduction in parental U-2 OS cells. In these experiments, overexpression of *GPR108* in parental cells did not further increase AAV transduction (Figure 6B). We then examined whether *GPR108* overexpression could rescue AAV transduction in *KIAA0319L* KO cells. KO of *KIAA0319L* reduced virus-mediated EGFP expression by 9.2-fold compared to parental cells ($p < 0.0001$), and stable overexpression

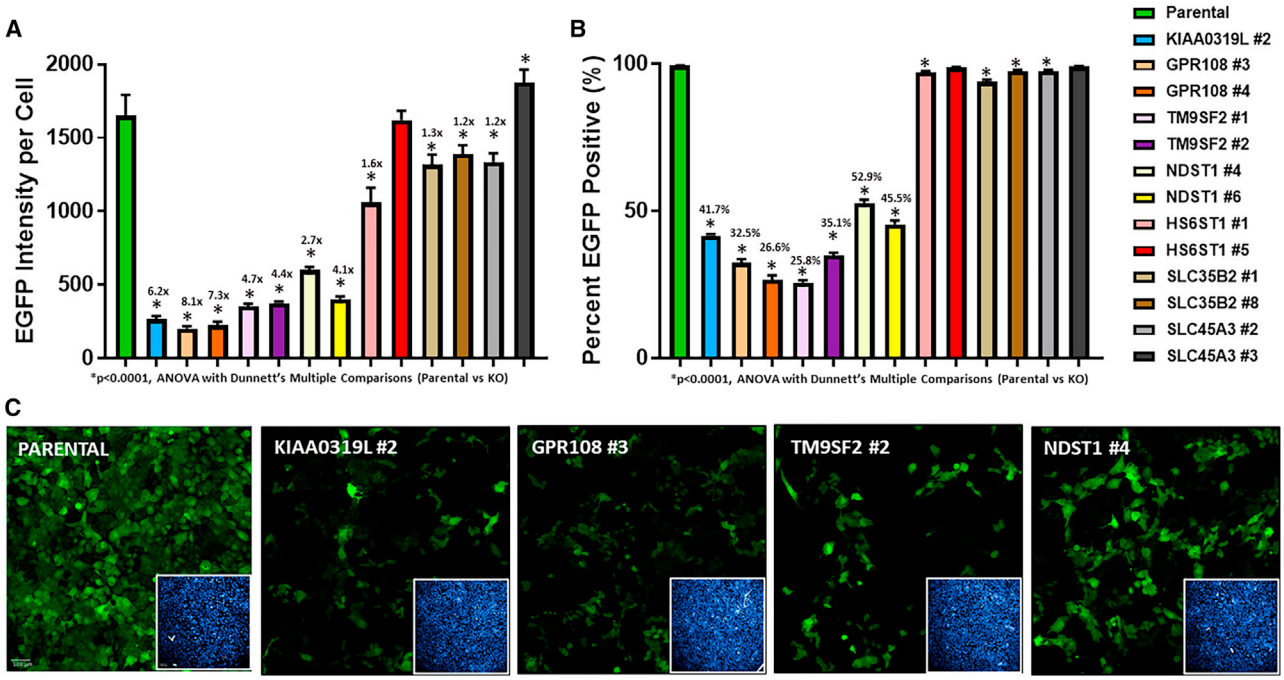

Figure 3. Validation of Genes Identified from the CRISPR/Cas Genome-wide Screen

U-2 OS KO cells were transduced with AAV2-EGFP at an MOI of 12,000. Parental U-2 OS cells were used as a positive control for EGFP expression, and *KIAA0319L* KO cells were used a negative control for EGFP expression. 3 days post-transduction the cells were fixed and imaged. (A) Average EGFP intensity per cell was quantified. (B) Percentages of EGFP-positive cells in imaged population were quantified. Data from bar graphs depict the mean value with SD (n = 5 wells/cell line; n = 9 fields/well). (C) Representative EGFP images from the experiment. Corresponding nuclear stains (Hoechst dye, blue) are shown in the inset.

of *GPR108* in these KO cells did not significantly increase AAV transduction compared *KIAA0319L* KO cells alone (Figure 6B).

GPR108 Localizes Primarily to the Golgi and It Is Ubiquitously Expressed in Most Tissues and Cell Types

GPR108 is seven-pass transmembrane protein, and it is predicted by the Human Protein Atlas (https://www.proteinatlas.org/) to localize to the Golgi and intracellular vesicles.[10] To evaluate the localization of the protein we utilized the U-2 OS cells expressing the epitope-tagged GPR108 generated earlier (Figure 6C). Cells were fixed and probed with a FLAG antibody. Images of stained cells suggested a predominantly perinuclear localization (Figures S5A and S5B). Dong et al.[11] previously reported GPR108 to be localized to the Golgi compartment. We confirmed this reported cellular localization using a BacMam reagent encoding the Golgi marker *N*-acetylgalactosaminyltransferase fused with EGFP (Figure 6D). As part of the infection process, AAV traffics to the Golgi and given the localization of GPR108, we examined colocalization of GPR108 and AAV within the cell.[12–14] For these experiments, HeLa cells were transfected with a *GPR108*-GFP fusion construct and treated with AAV2 containing mCherry fluorescent protein in its capsid (Figure 6C). Six hours post-transduction, cells were fixed and imaged, and a qualitative assessment suggested that GPR108 and AAV have a similar cellular localization (Figure 6E). These studies also confirmed the localization of GPR108 in a second cell line. In addition to conducting image-based cellular localization experiments, we also reviewed publicly available proteomics data to determine whether *GPR108* or *TM9SF2* might localize to the cell surface. An analysis of the mass spectrometric-derived cell surface protein atlas did not identify either protein on the cell surface of 41 different human cell types.[15] While not definitive, these findings suggest that if these proteins are present on the cell surface, they are most likely not very abundant in the cell types evaluated. In addition to defining the cellular localization of *GPR108*, we also examined its expression in a variety of different tissues and cell types. *GPR108* was ubiquitously expressed in most cell types and tissues (Genotype-Tissue Expression [GTex] Project), suggesting that *GPR108* may play a role in mediating AAV transduction in most tissue types.

DISCUSSION

Pooled CRISPR-Cas9 screens are powerful tools for dissecting complex biological processes such as viral infection. In this study we conducted two independent, pooled CRISPR screens in U-2 OS cells. We observed substantial agreement between the 155K library, the 80K library, and the Pillay et al.[1] HAP1 insertional mutagenesis study with all three screens identifying *TM9SF2*, *KIAA0319L*, and *GPR108* as highly significant genes required for AAV2 transduction. The fact that the same genes were identified using different genomic perturbation strategies in a haploid, Chronic Myelogenous Leukemia (CML)-derived line and an osteosarcoma line strongly suggests that these gene products are broadly required for AAV transduction.

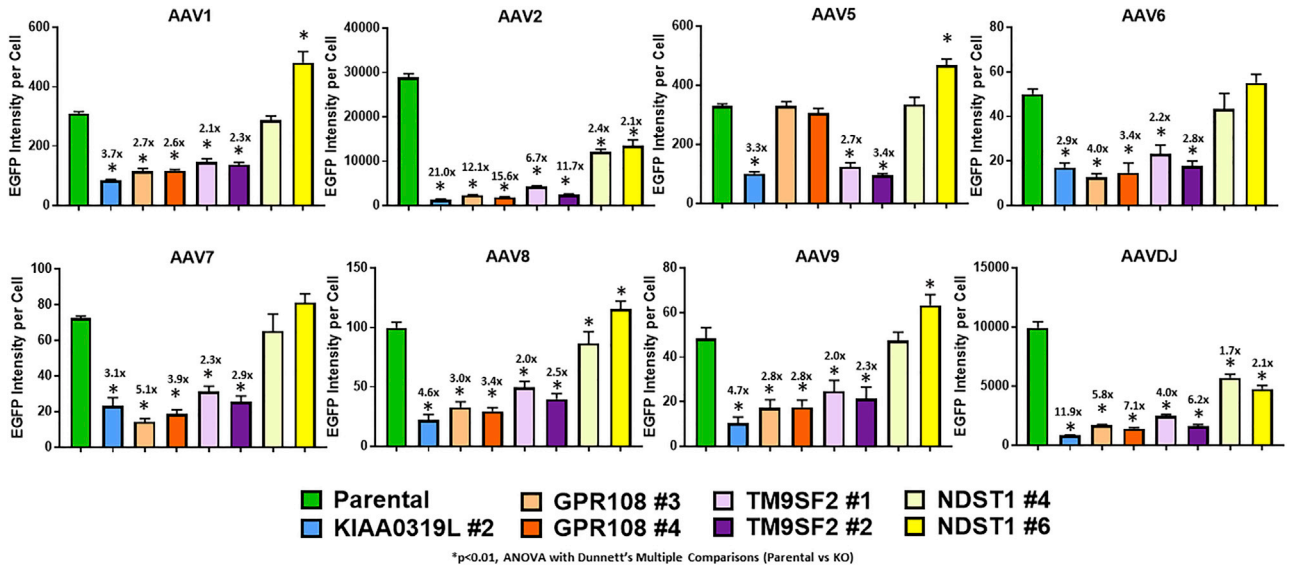

Figure 4. *GPR108* and *TM9SF2* Are Critical Host Cells Factors for AAV Transduction in Multiple Serotypes

U-2 OS KO cells were transduced with different AAV serotypes. Parental U-2 OS cells were used as a positive control for EGFP expression, and *KIAA0319L* KO cells were used a negative control for EGFP expression. 3 days post-transduction the cells were fixed and imaged. The mean EGFP intensity of cells in the imaged population was quantified. Data from bar graphs depict the mean value with SD (n = 5 wells/cell line; n = 9 fields/well).

Beyond the cell type and genomic perturbation strategy, we also took a different approach to identify genes involved in AAV2 transduction than that of Pillay et al.[1] In their study, they performed very stringent selection involving two rounds of sorting for transgene-negative (red fluorescent protein [RFP] in their study) cells. In this study, we piloted a different selection strategy using a high/low quartile sorting approach and compared it to a positive/negative strategy. We found that while both approaches produced correlated gene-level depletion or enrichment, the larger fold changes in the high/low sort improved the ability to detect significant depletions or enrichments and demonstrate one of the advantages of FACS-based pooled screens.[16] A further potential benefit of this high/low quartile sorting approach is that it is simultaneously capable of identifying both enriched and depleted genes. While there were no overlapping, significant genes in the two screens that improved AAV transduction, several genes that have been shown to be involved in AAV transduction such as *MRE11* and *RAD50* were identified as significant hits in the 155K screen.[17] Future studies will explore the mechanisms by which the perturbation of these genes may enhance AAV transduction.

We observed multiple significant hits in heparan sulfate (HS) synthesis pathways in both pooled screens. This result was not surprising, as membrane-associated HS proteoglycans (HSPGs) are thought to be important for AAV2 attachment and infection.[18] Indeed, HSPGs act as attachment receptors or co-receptors for entry of many viruses, including herpes simplex virus, dengue virus, human papillomavirus, human immunodeficiency virus, and adenovirus.[19] *EXT1*, *EXT2*, *HS6ST1*, *NDST1*, *SLC35B2*, and *TM9SF2* were among the top HS synthesis genes identified. *EXT1* and *EXT2* are important for HS chain formation and extension, and the absence of these exostosin glycosyltransferases have been shown to disrupt HS synthesis.[20–23] The enzyme *NDST1* introduces *N*-sulfate groups to the HS chain during elongation and interacts closely with *EXT2*.[24,25] *SLC35B2*, a member of the solute carrier family 35, transports 3′-phosphoadenosine-5′-phosphosulfate to act as a substrate for sulfation and thus enables NDST enzyme activity.[26–29] In this study, we observed *NDST1* reduced AAV-mediated EGFP expression but did not inhibit the percentage of cells that were transduced with AAV at a high MOI. Additional studies in KO cells confirmed that *NDST1* is important for AAV transduction in AAV2 and AAVDJ, but its role appeared to be MOI-dependent, as it was not required for successful transduction at high MOI in our experiments. Given the role of HSPGs on AAV2 and AAVDJ attachment, it was not surprising that *NDST1* KO reduced AAV transduction in these serotypes.[30,31] Interestingly, we did not observe a difference in transduction for AAV6 in *NDST1* KO cells. AAV6 is thought to utilize both HSPGs and sialic acid during the process of attachment, and it is possible we did not observe changes in AAV6 transduction due to its ability to use multiple cell surface molecules for cell attachment.[32,33] Alternatively, the overall transduction efficiency of AAV6 in U-2 OS cells was low even at high MOIs, which may have restricted the window needed to observe subtler differences in transduction we observed with *NDST1* KO. *TM9SF2* has been shown to be important for the stabilization and localization of *NDST1*.[4] Additionally, *TM9SF2* has previously been reported to localize to the Golgi where it is also involved in glycosphingolipid regulation and endosomal trafficking.[4,34,35] These additional functions of TM9SF2 may explain why TM9SF2 KO inhibited transduction in serotypes not dependent on HSPGs for infection. Given its major role in these processes, it is also not surprising that *TM9SF2* was among the strongest hits. Indeed, *TM9SF2* has also

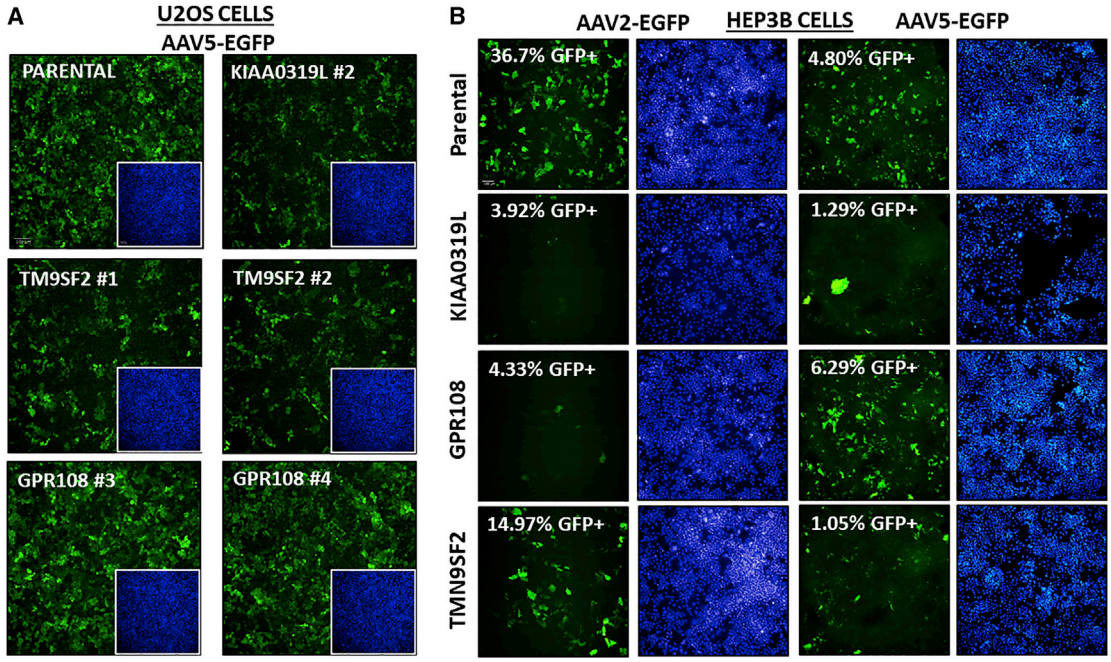

Figure 5. *GPR108* Is Not Required for AAV5 Transduction

(A) U-2 OS KO cells were transduced with AAV5-EGFP at an MOI of 55,000. 3 days post-transduction the cells were fixed and imaged. Representative EGFP images from the experiment are shown. Corresponding nuclear stains (Hoechst dye; blue) are shown in the inset. (B) HEP3B KO cells were transduced with AAV2-EGFP or AAV5-EGFP at an MOI of 18,000 or 55,000, respectively. 2 days post-transduction the cells were fixed and imaged. Representative EGFP images from the experiment are shown with corresponding nuclear stains in the adjacent image (AAV2 DRAQ5 stain, pseudo-color blue; AAV5, Hoechst dye). The percentage of EGFP-positive cells in the imaged population was quantified. The mean value is shown in the upper left corner (white) (AAV2: n = 2 wells/cell line; n = 9 fields/well; AAV5: n = 1 well/cell line; n = 9 fields/well). In both experiments parental cells were used as a positive control for EGFP expression, and *KIAA0319L* KO cells were used a negative control for EGFP expression.

been shown to be important for vaccinia virus infection, chikungunya virus infection, Shiga toxin activity, and ricin activity.[3] Single-nucleotide polymorphisms in *TM9SF2* are also associated with AIDS progression though unknown mechanisms.[36] This is one of the first studies to validate *TM9SF2* as a factor important for AAV transduction.

Among our significant hits, *GPR108* was perhaps the most interesting. *GPR108* is a putative G-protein-coupled receptor with no defined ligand and is similar to *KIAA0319L* (*AAVR*) in that very little is known about *GPR108*. Also known as *LUSTR2*, GPR108 has an amino-terminal hydrophobic signal peptide sequence, a large extracellular domain, and a carboxy-terminal seven-transmembrane domain.[37] The protein was previously linked to nuclear factor κB (NF-κB) signaling in a NF-κB reporter screen of 14,500 full-length mouse and human genes.[38] Of the 154 genes found to regulate NF-κB signaling, *GPR108* ranked among the top 20 genes in the luciferase reporter assay used in that study. Forced expression of *GPR108* has also been found to induce cytotoxicity, although it is unclear whether this finding results from strong NF-κB activation or another unidentified mechanism.[11] Indeed, we also observed that maintenance of stable or transient overexpression of *GPR108* was difficult in some of the cell lines we tested. While *GPR108* overexpression appears to be a potent activator of NF-κB, recent work suggests at low, physiological levels the protein may actually attenuate Toll-like receptor (TLR)-mediated immune responses. Dong et al.[11] observed that *GPR108* KO macrophages stimulated with TLR agonists had higher NF-κB activation and more cytokine production than did wild-type cells. In co-immunoprecipitation experiments, the authors found that GPR108 could interact with TRAF6 and multiple TLRs. The authors speculate that GPR108 may help in tempering immune responses induced via TLR activation. While this research indicates that *GPR108* plays an important role in NF-κB signaling, our study suggests it is also a critical regulator of multiple processes such as virus transduction.

GPR108's localization in the Golgi puts it in a setting to potentially interact with AAV. While we demonstrated that both GPR108 and AAV localize to the Golgi, we did not confirm GPR108's physical interaction with AAV. Future studies will confirm whether AAV binds to GPR108 or whether GPR108 modifies the Golgi environment to mediate efficient AAV trafficking and/or virus escape. Interestingly, AAV5 did not require GPR108 for efficient transduction. AAV5 is highly divergent from other AAVs and these differences are illustrated in the distinct interactions of AAV5 capsid with the PKD1 domain of *KIAA0319L*.[2,39,40] The unique characteristics of the AAV5 capsid may also dictate its potential interactions with proteins such as GPR108. AAV5 is reported to travel to the Golgi so it is

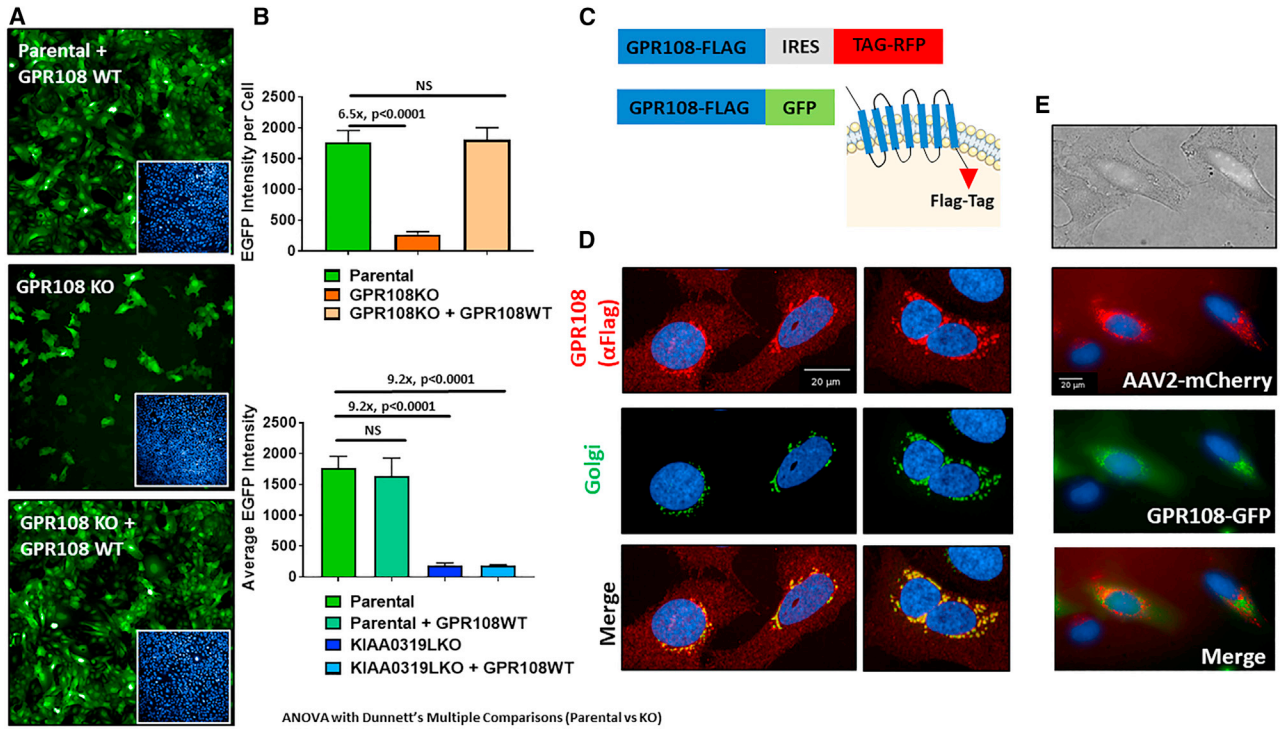

Figure 6. *GPR108* Predominantly Localizes to the Golgi, and *GPR108* Expression Is Not Sufficient to Rescue AAV Transduction in *KIAA0319L* KO Cells

U-2 OS parental, *GPR108*, and *KIAA0319L* KO cells expressing WT *GPR108* were generated. Modified cells were transduced with AAV2-EGFP at an MOI of 12,000. 3 days post-transduction the cells were fixed and imaged. (A) Representative EGFP images from the *GPR108* rescue experiment. Corresponding nuclear stains (Hoechst dye, blue) are shown in the inset. (B) The average EGFP intensity per cell was quantified from the rescue and overexpression experiments. Data from bar graphs depict the mean value with SD (n = 3 wells/cell line) (C) Left: graphical depictions of the expression cassettes used to perform the rescue and imaging experiments. Right: illustration of *GPR108* with a C-terminal FLAG-tag. (D) Parental U-2 OS cells expressing the *GPR108*-FLAG protein were fixed and stained. Representative images depict localization of FLAG-tag *GPR108* (red), Golgi (green), and Nuclei (blue). (E) HeLa cells expressing the *GPR108*-FLAG-GFP protein were transduced with AAV2-mCherry-capsid. After 6 h the cells were fixed and stained. Representative images depict localization of *GPR108*-FLAG-GFP (green), AAV2 (red), and nuclei (blue).

interesting that the virus does not require GPR108 for successful transduction.[14] During the completion of this study, a second group also validated GPR108 as a host cell factor important for AAV transduction. Dudek et al.[41] conducted a genome-wide CRISPR screen using the evolutionary divergent, AAVR-independent serotype AAVrh32.33 to identify highly conserved AAV entry factors. Similar to our findings, they found that Golgi-localized GPR108 was a critical factor for AAV transduction. While no mechanism was identified, they also observed that AAV5 did not require GPR108 for successful transduction. Further studies will elucidate the regulatory pathways that permit AAV5 transduction independent of GPR108 and a larger role of GPR108 in AAV transduction. In conclusion, these findings suggest that *GPR108* and *TM9SF2* are highly conserved factors critical for efficient AAV transduction across multiple serotypes.

MATERIALS AND METHODS

Cells and Viruses

U-2 OS were obtained from ATCC (Manassas, VA, USA). HeLa, Hep3B, and HEK293T cells were obtained from Amgen Discovery Research (South San Francisco, CA, USA). U-2 OS cells were maintained in McCoy's 5A media (Corning) containing 10% fetal bovine serum (FBS) (Sigma) and 1% penicillin-streptomycin (PS) solution (Corning). HeLa cells were maintained in DMEM (Corning) containing 10% FBS (Sigma) and 1% PS solution (Corning). Hep3B cells were maintained in Eagle's minimum essential medium (EMEM from ATCC 30-2003) with 10% FBS. Hep3B-Cas9 cells were also maintained in 10 μg/mL blasticidin. Suspension-adapted HEK293 cells were maintained in FreeStyle 293 expression medium containing GlutaMAX-I (Gibco), 2% FBS (Gibco), and G418 (Gibco). HeLa cells were maintained in DMEM (Corning) containing 10% FBS (Sigma) and 1% PS solution (Corning). All cells were cultured at 37°C with 5% CO_2. Viruses were generated in a suspension of 293T cells by the triple transfection method using PEI MAX (Polysciences). Viruses were purified by iodixanol gradient or affinity columns using POROS CaptureSelect AAV8, AAV9, or AAVX. Virus titer was determined using a QuickTiter AAV quantitation kit (Cell Biolabs) according to the manufacturer's instructions. AAV2-mCherry was made as previously described.[42] The plasmid ratio of VP1-mCherry/VP2+VP3 was 1:1.

CRISPR-Cas9 Genome-wide Screens

We generated a Cas9-expressing stable pool by transducing U-2 OS cells with the viral vector pCLIP-Cas9-Nuclease-EFS-Blast

(Transomic Technologies) packed into vesicular stomatitis virus G protein (VSV-G) pseudotyped virions followed by selection with blasticidin S (Gibco) at a concentration of 5 μg/mL for 14 days. The resistant pool of U-2 OS cells was subsequently transduced with one of four CRISPR libraries, that is, CRISPR human genome KO library modules 1, 2, or 3 or the 80K genome-wide library (Cellecta, Mountain View, CA, USA). All four libraries use the same pRSG16-U6-sg-UbiC-TagRFP-2A-Puro vector, which express both the puromycin resistance marker as well as RFP for determination of titer. Library transductions were targeted to MOIs ranging from 0.25 to 0.4 with coverage (average number of cells per library element) of between 384 and 900. Three days after transduction, aliquots of cells were harvested, washed, fixed in 2% formaldehyde (Sigma), and assessed for RFP fluorescence on the LSR II cytometer (BD). Based on the percentage of positive cells, we estimated the MOI and coverage, and the range of those numbers can be found in Figure 1A. The transduced cells were subsequently selected with both blasticidin and puromycin (Gibco) to maintain expression of Cas9 and sgRNA until day 14 post-transduction.

For both the pilot and genome-wide screens, on day 14 cells were seeded in 1,000× coverage replicates (i.e., 8e7 cells for the 80K library) in fresh, non-selective, complete media. One day later, AAV2-EGFP virus was added at a 0 (mock), 60, or 1,200 MOI in antibiotic-free media supplemented with 1% serum. The following day, the media were replaced with standard, antibiotic-free media. Three days after AAV transduction, the cells were harvested, counted, washed, and fixed in 2% formaldehyde. After fixation, transduced samples were sorted as described on a FACSAria III (BD Biosciences). In general, we collected 10–20 million cells in each gate from a starting population of greater than 200 million cells.

Genomic DNA was extracted from sorted and unsorted (mock) samples using the Gentra Puregene tissue kit. The yield and quality of extracted DNA was assessed with the NanoDrop One (Thermo Fisher Scientific, Waltham, MA, USA). All of the DNA from the sorted samples along with DNA from ~100 million mock-transduced cells was sent to Cellecta for barcode amplification and enumeration by NGS.

Individual samples were all arbitrarily normalized to 50 million reads. For statistical analysis, sgRNA abundance in the mock sample was compared to initial abundance in the plasmid library and sorted samples were compared as described. Individual sgRNAs with fewer than 50 counts were filtered prior to calculating ratios that were subsequently transformed into ranks and rank fractions. Rank fractions were transformed into *Z* scores and a raw p value calculated by multiplying the square root of the number of sgRNAs for a given gene by the mean *Z* score. p values were then converted to FDR using the Benjamini-Hochberg method.

KO Cell Line Generation

Stable U-2 OS KO cell lines were generated using lentivirus encoding Cas9, an sgRNA to a target gene, and a puromycin selection marker. Constructs, sgRNAs, and viruses were created by Cellecta. Parental U2-OS cells were transduced at an MOI of 1 and selected with puromycin (2 μg/mL) for 6 days (10 days post-transduction). To generate HEP3B KO cell lines, Cas9 stable Hep3B cells were transfected with three multiplexed sgRNAs (Synthego, Menlo Park, CA, USA) using Lipofectamine CRISPRMAX (Thermo Fisher Scientific). The transfected cells were cultured for 6 days prior to the AAV transduction assay. Gene KO was estimated via ICE analysis (Synthego) of Sanger sequencing data.

AAV-EGFP Transduction Assays

12,000 U-2 OS parental or KO cells were plated in 96-well plates in McCoy's media containing 10% FBS. For U-2 OS assays with rAAV2-EGFP, the cells were transduced the following day at 12,000 genome copies (gc)/cell. For U-2 OS assays comparing the impact of gene KO on rAAV transduction with other serotypes of rAAV, an average MOI of 100,000 was used. Transduced cells were fixed 3 days post-transduction with 2% paraformaldehyde (PFA) and stained with Hoechst dye to visualize cell nuclei. For studies with HEP3B cells, ~20,000 cells were transduced at an MOI of 18,000 or 55,000 for AAV2-EGFP and AAV5-EGFP, respectively. Transduced cells were fixed 3 days post-transduction with 2% PFA and stained with Hoechst dye or DRAQ5 to visualize cell nuclei. Images were acquired on an Opera Phenix (PerkinElmer) and analyzed in Columbus (version 2.9.0.1546) and TIBCO Spotfire Analyst (version 7.6.1). Statistical analyses were performed in GraphPad Prism 7.05. Student's t tests or ANOVA with Dunnett's or Bonferroni multiple comparisons tests were performed where appropriate. $p < 0.05$ was considered significant.

GPR108 Rescue Experiments

U-2 OS cells were seeded at a density of 360,000 cells per six wells in 1 mL of 10% FBS McCoy's medium. Transduction was performed with viral stock in a total of 3 mL of medium with Polybrene (8 μg/mL). Plates were shaken gently and placed back in the incubator and incubated at 37°C and 5% CO_2. 72 h post-transduction, transduction efficiency was evaluated by measuring the percentage of RFP-expressing cells by flow cytometry and analyzed by FlowJo software. Cells were sorted based on RFP expression profile and were cultured for 1 week. For rescue experiments, U-2 OS cells stably expressing *GPR108*-FLAG constructs were plated at 12,000 cells/well in a 96-well plate and were transduced with AAV2-EGFP at an MOI of 12,000. Three days later, cells were fixed in 4% PFA for further immunofluorescence analysis.

Immunofluorescence Experiments

For GPR108 localization studies, U-2 OS cells stably expressing or transfected with a *GPR108*-FLAG construct were fixed with 4% PFA, permeabilized with 0.3% Triton X-100, and blocked with 0.2% bovine serum albumin proteins (BD Pharmingen). The cells were probed with mouse anti-FLAG antibody (Sigma, F1804) and visualized with Alexa Fluor 488 (Thermo Fisher Scientific, A11032) or Alexa Fluor 647 (Thermo Fisher Scientific, A32728) goat anti-mouse secondary antibodies. Secondary antibodies were applied in the presence of 0.1% Triton X-100. For Golgi localization studies, cells were

treated 24 h prior to fixation with BacMam 2.0 CellLight reagents to visualize Golgi (*N*-acetylgalactosaminyltransferase-GFP, Molecular Probes, C10592) and late endosomes (Rab7a-GFP, Molecular Probes, C10588). For AAV co-localization studies, HeLa cells were transduced in cold media with AAV2-mCherry at an MOI of 1.44×10^6 for 2.5 h, then washed twice with warm 10% FBS containing DMEM to remove unbound virus, and incubated for an additional 4 h at 37°C. After 6 h the cells were fixed and imaged.

SUPPLEMENTAL INFORMATION

Supplemental Information can be found online at https://doi.org/10.1016/j.omtm.2020.03.012.

AUTHOR CONTRIBUTIONS

Conceptualization, W.H.M., M.O., S.W., and P.C.; Methodology, W.H.M., Z.B.N., M.H., H.Z., O.O., C.H., and P.C.; Resources, W.H.M. and H.Z.; Investigation, W.H.M., Z.B.N., M.H., and P.C.; Writing – Original Draft, W.H.M., Z.B.N., H.Z., M.O., and P.C.

CONFLICTS OF INTEREST

Authors are current or former employees of Amgen, Thousand Oaks, CA, USA.

ACKNOWLEDGMENTS

This work was supported by Amgen Discovery Research (South San Francisco, CA, USA). The Genotype-Tissue Expression (GTEx) Project was supported by the Common Fund of the Office of the Director of the National Institutes of Health, and by NCI, NHGRI, NHLBI, NIDA, NIMH, and NINDS. The data used for the analyses described in this manuscript were obtained from the GTEx Portal (on August 1, 2019) and/or dbGaP: phs000424.vN.pN (on August 1, 2019). We thank Servier Medical for images used to create Figure 6. Servier Medial Art by Servier is licensed under a Creative Commons Attribution 3.0 Unported License.

REFERENCES

1. Pillay, S., Meyer, N.L., Puschnik, A.S., Davulcu, O., Diep, J., Ishikawa, Y., Jae, L.T., Wosen, J.E., Nagamine, C.M., Chapman, M.S., and Carette, J.E. (2016). An essential receptor for adeno-associated virus infection. Nature *530*, 108–112.

2. Pillay, S., Zou, W., Cheng, F., Puschnik, A.S., Meyer, N.L., Ganaie, S.S., Deng, X., Wosen, J.E., Davulcu, O., Yan, Z., et al. (2017). Adeno-associated virus (AAV) serotypes have distinctive interactions with domains of the cellular AAV receptor. J. Virol. *91*, e00391-17.

3. Luteijn, R.D., van Diemen, F., Blomen, V.A., Boer, I.G.J., Manikam Sadasivam, S., van Kuppevelt, T.H., Drexler, I., Brummelkamp, T.R., Lebbink, R.J., and Wiertz, E.J. (2019). A genome-wide haploid genetic screen identifies heparan sulfate-associated genes and the macropinocytosis modulator TMED10 as factors supporting vaccinia virus infection. J. Virol. *93*, e02160-18.

4. Tanaka, A., Tumkosit, U., Nakamura, S., Motooka, D., Kishishita, N., Priengprom, T., Sa-Ngasang, A., Kinoshita, T., Takeda, N., and Maeda, Y. (2017). Genome-wide screening uncovers the significance of *N*-sulfation of heparan sulfate as a host cell factor for chikungunya virus infection. J. Virol. *91*, e00432-17.

5. Carette, J.E., Guimaraes, C.P., Varadarajan, M., Park, A.S., Wuethrich, I., Godarova, A., Kotecki, M., Cochran, B.H., Spooner, E., Ploegh, H.L., and Brummelkamp, T.R. (2009). Haploid genetic screens in human cells identify host factors used by pathogens. Science *326*, 1231–1235.

6. Gerhards, N.M., and Rottenberg, S. (2018). New tools for old drugs: functional genetic screens to optimize current chemotherapy. Drug Resist. Updat. *36*, 30–46.

7. Yilmaz, A., Peretz, M., Sagi, I., and Benvenisty, N. (2016). Haploid human embryonic stem cells: half the genome, double the value. Cell Stem Cell *19*, 569–572.

8. Doench, J.G. (2018). Am I ready for CRISPR? A user's guide to genetic screens. Nat. Rev. Genet. *19*, 67–80.

9. Hsiau, T., Conant, D., Rossi, N., Maures, T., Waite, K., Yang, J., Joshi, S., Kelso, R., Holden, K., Enzmann, B.L., et al. (2018). Inference of CRISPR edits from Sanger trace data. bioRxiv. https://doi.org/10.1101/251082.

10. Thul, P.J., Åkesson, L., Wiking, M., Mahdessian, D., Geladaki, A., Ait Blal, H., Alm, T., Asplund, A., Björk, L., Breckels, L.M., et al. (2017). A subcellular map of the human proteome. Science *356*, eaal3321.

11. Dong, D., Zhou, H., Na, S.Y., Niedra, R., Peng, Y., Wang, H., Seed, B., and Zhou, G.L. (2018). GPR108, an NF-κB activator suppressed by TIRAP, negatively regulates TLR-triggered immune responses. PLoS ONE *13*, e0205303.

12. Nonnenmacher, M.E., Cintrat, J.C., Gillet, D., and Weber, T. (2015). Syntaxin 5-dependent retrograde transport to the *trans*-Golgi network is required for adeno-associated virus transduction. J. Virol. *89*, 1673–1687.

13. Nonnenmacher, M., and Weber, T. (2011). Adeno-associated virus 2 infection requires endocytosis through the CLIC/GEEC pathway. Cell Host Microbe *10*, 563–576.

14. Bantel-Schaal, U., Hub, B., and Kartenbeck, J. (2002). Endocytosis of adeno-associated virus type 5 leads to accumulation of virus particles in the Golgi compartment. J. Virol. *76*, 2340–2349.

15. Bausch-Fluck, D., Hofmann, A., Bock, T., Frei, A.P., Cerciello, F., Jacobs, A., Moest, H., Omasits, U., Gundry, R.L., Yoon, C., et al. (2015). A mass spectrometric-derived cell surface protein atlas. PLoS ONE *10*, e0121314.

16. Shifrut, E., Carnevale, J., Tobin, V., Roth, T.L., Woo, J.M., Bui, C.T., Li, P.J., Diolaiti, M.E., Ashworth, A., and Marson, A. (2018). Genome-wide CRISPR screens in primary human T cells reveal key regulators of immune function. Cell *175*, 1958–1971.e15.

17. Lentz, T.B., and Samulski, R.J. (2015). Insight into the mechanism of inhibition of adeno-associated virus by the Mre11/Rad50/Nbs1 complex. J. Virol. *89*, 181–194.

18. Summerford, C., and Samulski, R.J. (1998). Membrane-associated heparan sulfate proteoglycan is a receptor for adeno-associated virus type 2 virions. J. Virol. *72*, 1438–1445.

19. Cagno, V., Tseligka, E.D., Jones, S.T., and Tapparel, C. (2019). Heparan sulfate proteoglycans and viral attachment: true receptors or adaptation bias? Viruses *11*, E596.

20. Kreuger, J., and Kjellén, L. (2012). Heparan sulfate biosynthesis: regulation and variability. J. Histochem. Cytochem. *60*, 898–907.

21. Busse, M., Feta, A., Presto, J., Wilén, M., Grønning, M., Kjellén, L., and Kusche-Gullberg, M. (2007). Contribution of EXT1, EXT2, and EXTL3 to heparan sulfate chain elongation. J. Biol. Chem. *282*, 32802–32810.

22. Lind, T., Tufaro, F., McCormick, C., Lindahl, U., and Lidholt, K. (1998). The putative tumor suppressors EXT1 and EXT2 are glycosyltransferases required for the biosynthesis of heparan sulfate. J. Biol. Chem. *273*, 26265–26268.

23. McCormick, C., Duncan, G., Goutsos, K.T., and Tufaro, F. (2000). The putative tumor suppressors EXT1 and EXT2 form a stable complex that accumulates in the Golgi apparatus and catalyzes the synthesis of heparan sulfate. Proc. Natl. Acad. Sci. USA *97*, 668–673.

24. Presto, J., Thuveson, M., Carlsson, P., Busse, M., Wilén, M., Eriksson, I., Kusche-Gullberg, M., and Kjellén, L. (2008). Heparan sulfate biosynthesis enzymes EXT1 and EXT2 affect NDST1 expression and heparan sulfate sulfation. Proc. Natl. Acad. Sci. USA *105*, 4751–4756.

25. Dou, W., Xu, Y., Pagadala, V., Pedersen, L.C., and Liu, J. (2015). Role of deacetylase activity of *N*-deacetylase/*N*-sulfotransferase 1 in forming *N*-sulfated domain in heparan sulfate. J. Biol. Chem. *290*, 20427–20437.

26. Kamiyama, S., Suda, T., Ueda, R., Suzuki, M., Okubo, R., Kikuchi, N., Chiba, Y., Goto, S., Toyoda, H., Saigo, K., et al. (2003). Molecular cloning and identification of 3′-phosphoadenosine 5′-phosphosulfate transporter. J. Biol. Chem. *278*, 25958–25963.

27. Dick, G., Akslen-Hoel, L.K., Grøndahl, F., Kjos, I., Maccarana, M., and Prydz, K. (2015). PAPST1 regulates sulfation of heparan sulfate proteoglycans in epithelial MDCK II cells. Glycobiology *25*, 30–41.

28. Sasaki, N., Hirano, T., Ichimiya, T., Wakao, M., Hirano, K., Kinoshita-Toyoda, A., Toyoda, H., Suda, Y., and Nishihara, S. (2009). The 3′-phosphoadenosine 5′-phosphosulfate transporters, PAPST1 and 2, contribute to the maintenance and differentiation of mouse embryonic stem cells. PLoS ONE *4*, e8262.

29. Carlsson, P., Presto, J., Spillmann, D., Lindahl, U., and Kjellén, L. (2008). Heparin/heparan sulfate biosynthesis: processive formation of *N*-sulfated domains. J. Biol. Chem. *283*, 20008–20014.

30. Lerch, T.F., O'Donnell, J.K., Meyer, N.L., Xie, Q., Taylor, K.A., Stagg, S.M., and Chapman, M.S. (2012). Structure of AAV-DJ, a retargeted gene therapy vector: cryo-electron microscopy at 4.5 Å resolution. Structure *20*, 1310–1320.

31. Grimm, D., Lee, J.S., Wang, L., Desai, T., Akache, B., Storm, T.A., and Kay, M.A. (2008). In vitro and in vivo gene therapy vector evolution via multispecies interbreeding and retargeting of adeno-associated viruses. J. Virol. *82*, 5887–5911.

32. Wu, Z., Miller, E., Agbandje-McKenna, M., and Samulski, R.J. (2006). 2,α2,3 and α2,6 N-linked sialic acids facilitate efficient binding and transduction by adeno-associated virus types 1 and 6. J. Virol. *80*, 9093–9103.

33. Arnett, A.L., Beutler, L.R., Quintana, A., Allen, J., Finn, E., Palmiter, R.D., and Chamberlain, J.S. (2013). Heparin-binding correlates with increased efficiency of AAV1- and AAV6-mediated transduction of striated muscle, but negatively impacts CNS transduction. Gene Ther. *20*, 497–503.

34. Yamaji, T., Sekizuka, T., Tachida, Y., Sakuma, C., Morimoto, K., Kuroda, M., and Hanada, K. (2019). A CRISPR screen identifies LAPTM4A and TM9SF proteins as glycolipid-regulating factors. iScience *11*, 409–424.

35. Tian, S., Muneeruddin, K., Choi, M.Y., Tao, L., Bhuiyan, R.H., Ohmi, Y., Furukawa, K., Furukawa, K., Boland, S., Shaffer, S.A., et al. (2018). Genome-wide CRISPR screens for Shiga toxins and ricin reveal Golgi proteins critical for glycosylation. PLoS Biol. *16*, e2006951.

36. Chinn, L.W., Tang, M., Kessing, B.D., Lautenberger, J.A., Troyer, J.L., Malasky, M.J., McIntosh, C., Kirk, G.D., Wolinsky, S.M., Buchbinder, S.P., et al. (2010). Genetic associations of variants in genes encoding HIV-dependency factors required for HIV-1 infection. J. Infect. Dis. *202*, 1836–1845.

37. Edgar, A.J. (2007). Human GPR107 and murine Gpr108 are members of the LUSTR family of proteins found in both plants and animals, having similar topology to G-protein coupled receptors. DNA Seq. *18*, 235–241.

38. Halsey, T.A., Yang, L., Walker, J.R., Hogenesch, J.B., and Thomas, R.S. (2007). A functional map of NFκB signaling identifies novel modulators and multiple system controls. Genome Biol. *8*, R104.

39. Zhang, R., Xu, G., Cao, L., Sun, Z., He, Y., Cui, M., Sun, Y., Li, S., Li, H., Qin, L., et al. (2019). Divergent engagements between adeno-associated viruses with their cellular receptor AAVR. Nat. Commun. *10*, 3760.

40. Bantel-Schaal, U., Delius, H., Schmidt, R., and zur Hausen, H. (1999). Human adeno-associated virus type 5 is only distantly related to other known primate helper-dependent parvoviruses. J. Virol. *73*, 939–947.

41. Dudek, A.M., Zabaleta, N., Zinn, E., Pillay, S., Zengel, J., Porter, C., Franceschini, J.S., Estelien, R., Carette, J.E., Zhou, G., et al. (2020). GPR108 is a highly conserved AAV entry factor. Mol. Ther. *28*, 367–381.

42. Judd, J., Wei, F., Nguyen, P.Q., Tartaglia, L.J., Agbandje-McKenna, M., Silberg, J.J., and Suh, J. (2012). Random insertion of mCherry into VP3 Domain of Adeno-associated Virus Yields Fluorescent Capsids With no Loss of Infectivity. Mol. Ther. Nucleic Acids *1*, e54.